Electronic Supplementary Material (ESI) for Inorganic Chemistry Frontiers.

Supplementary information

Antagonist elastic interactions tuning spin crossover and LIESST behaviours in Fe(II) trinuclear-based one-dimensional chains

Narsimhulu Pittala,[a] Emmelyne Cuza,[a] Dawid Pinkowicz,[b] Michał Magott,[b] Mathieu Marchivie,[c] Kamel Boukheddaden,[d] Smail Triki[a]

[a]Univ Brest, CNRS, CEMCA, 6 Avenue Victor Le Gorgeu, C.S. 93837 - 29238 Brest Cedex 3, France
[b]Faculty of Chemistry, Jagiellonian University, Gronostajowa 2, 30-387 Kraków, Poland.
[c]CNRS, Univ. Bordeaux, Bordeaux INP, ICMCB, UMR 5026, 87 Avenue du Dr A. Schweitzer, F-33608 Pessac, France.
[d]Université Paris-Saclay, Université de Versailles Saint Quentin, CNRS, GEMaC UMR 8635, 45 Av. des Etats-Unis, 78035 Versailles Cedex, France.

1 - General Considerations and characterizations

All the starting reagents were purchased from commercial sources (Sigma-Aldrich, Across and Fisher Scientific) and used without further purification unless otherwise stated. Deuterated solvents were purchased from Sigma-Aldrich and Cambridge Isotope Laboratories. Dried solvents were prepared by refluxing for one day under dinitrogen over the appropriate drying agents (calcium hydride for hexane; magnesium and iodine for methanol; sodium for ethanol, and molecular sieves for DMF), and then degassed before use. Solvents were stored in glass ampoules under argon. Alternatively, they could be obtained from a solvent purification device (MBRAUN). When appropriate, the reactions were carried out under argon or nitrogen by using a dual manifold vacuum/argon line and standard Schlenk techniques. $^{1}H/^{13}C/^{31}P$-NMR spectra were recorded on Bruker AMX-300, AMX-400 and AMX-500 spectrometers, and the spectra were referenced internally using residual proton solvent resonances relative to tetramethylsilane (δ = 0 ppm). Temperature dependence of IR spectroscopy was performed, in the 2220-2200 cm^{-1} range, using a Vertex FT-IR BRUKER ATR VERTEX70 spectrometer with variable temperature cell holder (VT Cell Holder type P/N GS21525). The infrared spectra have been recorded using a KBr pellet painted with a tiny layer of nujol on which single crystals of the sample are sprinkled. A background was performed before sprinkling single crystals on the nujol KBr surface. In both cooling and warming scans, the IR spectra were collected after 5 minutes intervals and each temperature was stabilized during 1 min. Elemental analyses were performed at the "Service de microanalyse", CNRS, 91198 Gif-sur-Yvette, France. Thermogravimetric analysis (TGA) for **1·4H$_2$O** was performed under a nitrogen atmosphere using TG209 F1 Libra thermogravimetric analyzer (Netzsch) in the 20-90 °C range. Powder X-ray diffraction patterns were recorded at room temperature for sample loaded into 0.5 mm glass capillaries using Bruker D8 Advance Eco powder diffractometer equipped with a Cu Kα X-ray radiation source, a SSD160 LYNXEYE detector and a capillary spinning add-on.
Because of the use of organic ligands composed with cyano functional groups, all the experiments reported here have been undergone with great caution, especially considering the eventual release of the gases HCN and related derivatives that are poisonous and potentially lethal at low levels. Consequently, all those compounds should be prepared and handled behind suitable protective shields. In this context, all the waste involving polynitrile compounds were destroyed using a specific basic bath containing a saturated ethanolic solution of KOH mixed with an aqueous solution of NaOCl, while the glasswares were cleaned using a basic bath consisting of a saturated ethanol/water solution of KOH (1:1 volume ratio).

2 – Ligand Syntheses.

a) Synthesis of the functionalized triazole ligand. The 4-(benzyl)-1,2,4-triazole (bntrz) ligand was synthesized by modifying a previously reported method.[1-2] A solution of

formic hydrazide (1.8 g; 30 mmol) and triethyl orthoformate (6 mL, 36 mmol) in 30 mL of anhydrous methanol was refluxed for 8 hours. To the resulting light pink solution was added benzylamine (3.3 mL, 30 mmol) under nitrogen atmosphere at 55 °C, and then the mixture was further refluxed for 24 hours (see Scheme 1).

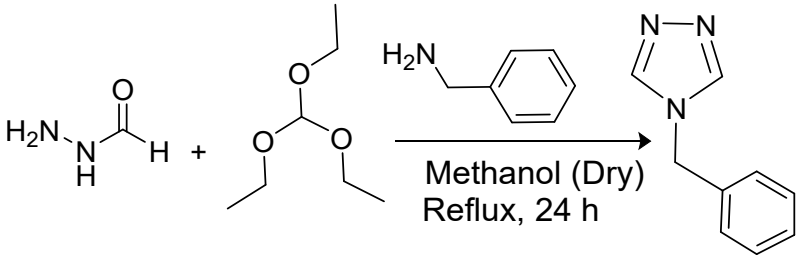

Scheme 1. Synthesis of the triazole derivative 4-(Benzyl)-1,2,4-triazole (bntrz).

After removal of the solvent under reduced pressure, the crude product was extracted with dichloromethane, washed with brine and dried over magnesium sulfate before being recrystallized from methanol and ether to obtain the triazole ligand as a white crystalline solid (Yield: 3.1 g, 65 %). ^{1}H NMR (500 MHz, $CDCl_3$, 298 K, *δ (ppm)*): 5.07 (s, 2H, CH_2), 7.06-7.09(m, 2H, CH), 7.25-7.28 (m, 3H, CH), 8.06 (s, 2H, CH=N), Fig. S1. ^{13}C NMR (75 MHz, $CDCl_3$, 298 K, *δ (ppm)*): 48.8 (Ar-C-N), 127.4 (Ar-C), 128.7 (Ar-C), 129.1(Ar-C), 134.1 (Ar-C), 142.7(N-C=N), Fig. S2. H-H COSY, NMR (500 MHz, $CDCl_3$, 298 K, *δ (ppm)*): see Fig. S3. H-C HMQC, NMR (500 MHz, $CDCl_3$, 298 K, *δ (ppm)*): see Fig. S4. H-C HMBC, NMR (500 MHz, $CDCl_3$, 298 K, *δ (ppm)*): Fig. S5. IR (ν, cm^{-1}): 3129w, 3084w, 3029w, 2972w, 1679w, 1534w, 1519w, 1496w, 1454w, 1379w, 1365w, 1338w, 1207w, 1181m, 1074w, 1031w, 1001w, 975w, 957w, 891w, 841w, 816w, 768w, 711s, 690m, 638m, 615w, 578w, 460w (Fig. S6).

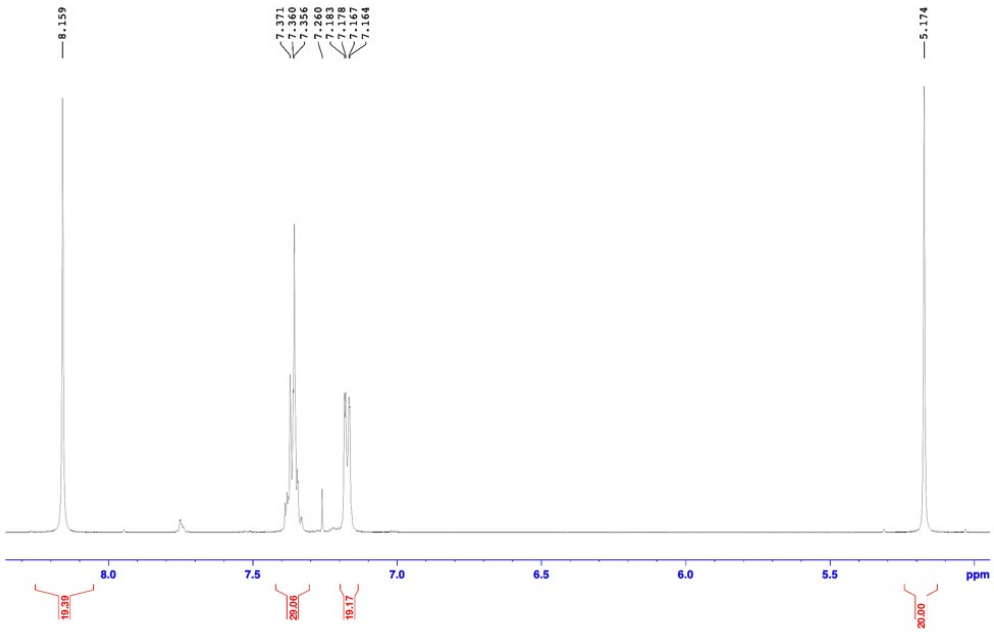

Figure S1. ^{1}H NMR (500 MHz, $CDCl_3$, 298K) of 4-(benzyl)-1,2,4-triazol (bntrz)

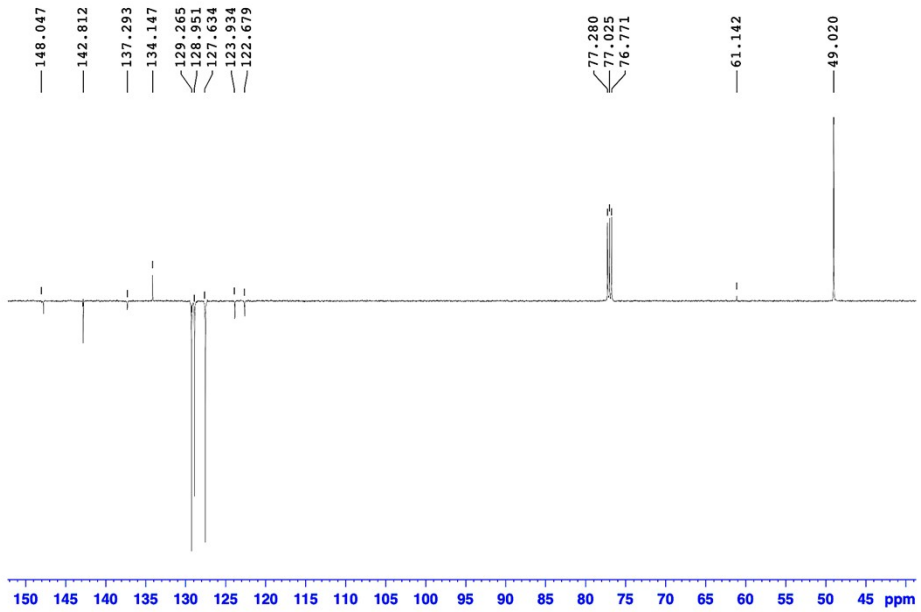

Figure S2. ^{13}C NMR (300 MHz, $CDCl_3$, 298 K) of 4-(benzyl)-1,2,4-triazol (bntrz)

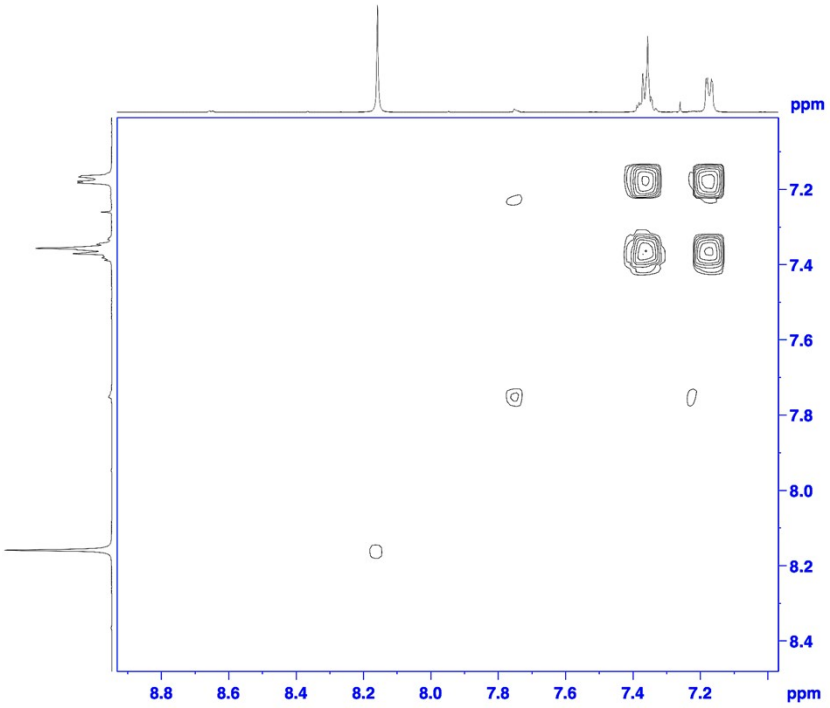

Figure S3. H-H COSY, NMR (500 MHz, $CDCl_3$) δ(ppm) of 4-(benzyl)-1,2,4-triazol

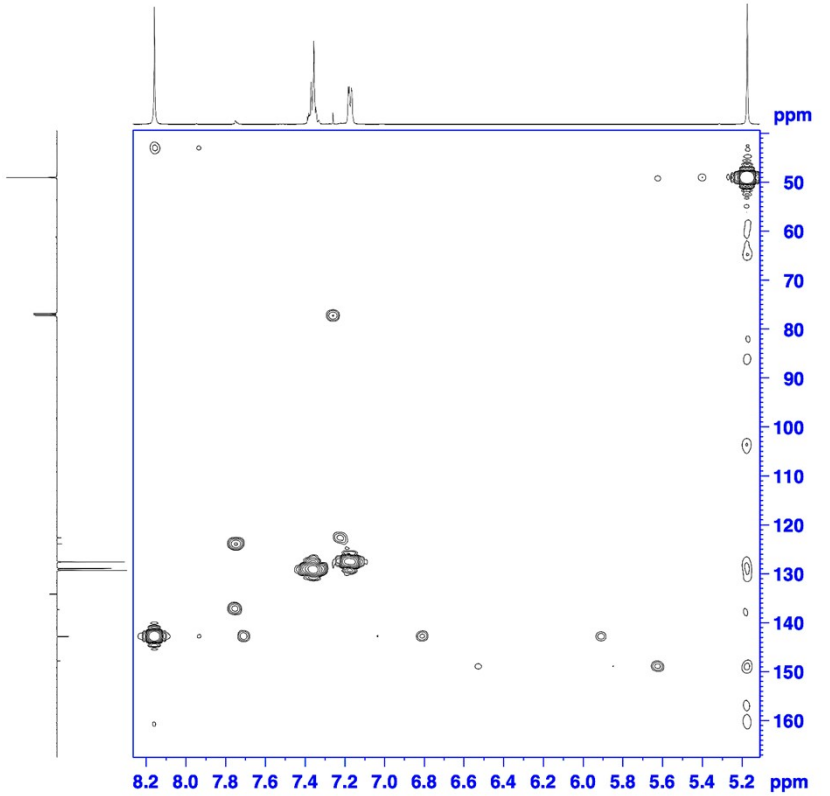

Figure S4. H-C HMQC, NMR (500MHz, $CDCl_3$) δ(ppm) of 4-(benzyl)-1,2,4-triazol

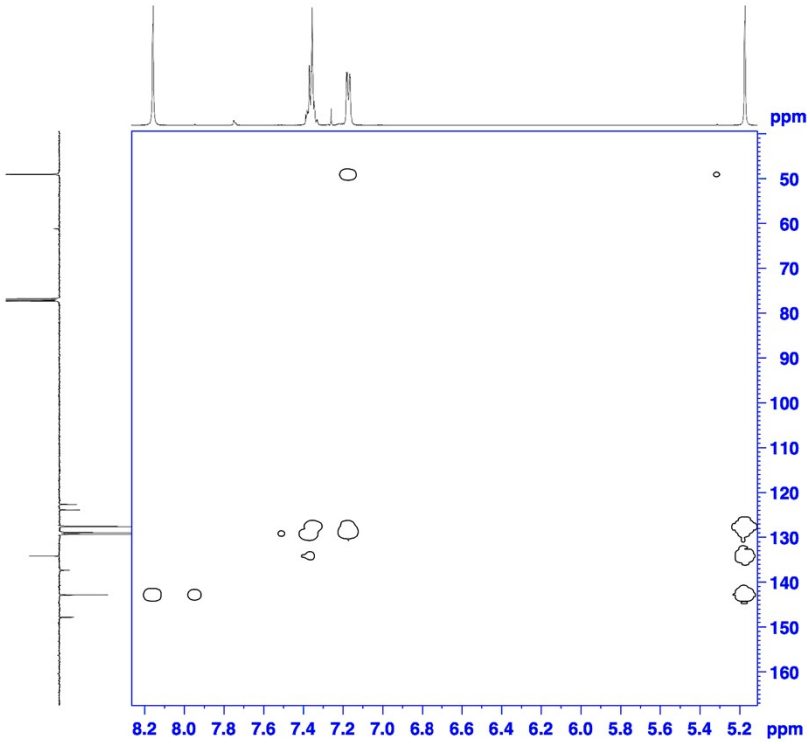

Figure S5. H-C HMBC, NMR (500 MHz, $CDCl_3$) δ(ppm) of 4-(benzyl)-1,2,4-triazol

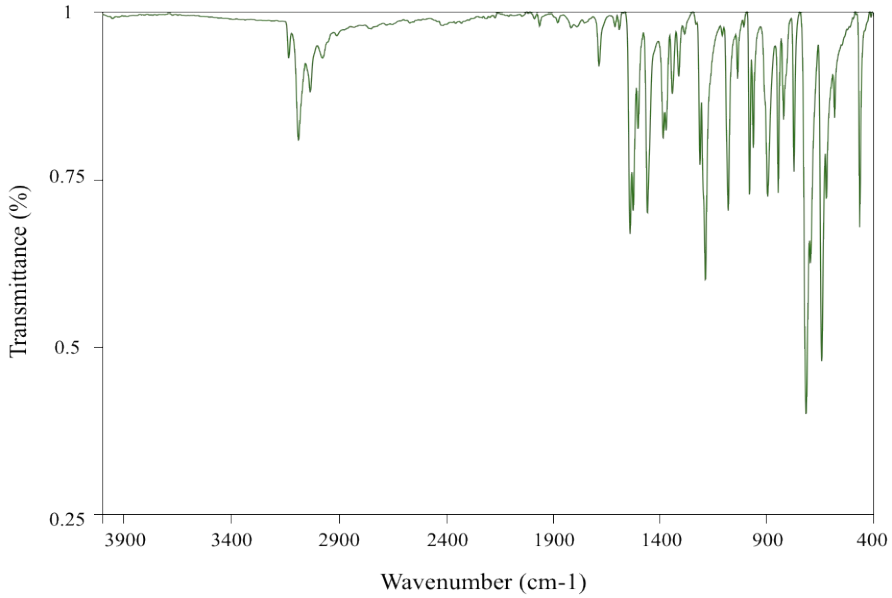

Figure S6. Infrared Spectrum of 4-(benzyl)-1,2,4-triazol (bntrz), IR data (ν, cm^{-1}): 3129m, 3084w, 3029w, 2972w, 1809w, 1782w, 1746w, 1679w, 1604w, 1584w, 1534s, 1519s, 1496m, 1453m, 1379m, 1365m, 1337w, 1306w, 1278w, 1207w, 1181s, 1103w, 1074m, 1031w, 1001w, 975m, 957m, 891m, 841m, 816w, 768m, 711s, 690s, 638s, 615m, 578w, 460m.

b) Synthesis of the cyanocarbanion coligand. The 1,1,3,3-tetracyano-2-thiomethylpropenide cyanocarbanion was prepared as potassium salt the two following steps (see Scheme 2):[3]

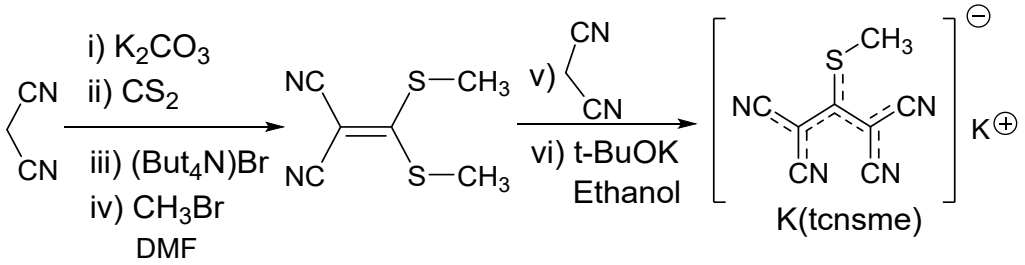

Scheme 2. Synthesis of potassium 1,1,3,3-tetracyano-2-thiomethylpropenide salt (K(tcnsme)).

(i) 2-[bis(methylthio)methylene]malononitrile. A suspension of K_2CO_3 (8.37 g, 60.55 mmol) in DMF (25 mL) was treated with the addition of malononitrile (4.0 g, 60.55 mmol). The mixture was cooled down to 0 °C, and CS_2 (3.6 mL, 66.6 mmol) was added dropwise. The resulting yellow suspension was stirred at 20 °C for 10 minutes, after which methyl bromide (11.50 g, 121.1 mmol) and tetrabutylammonium bromide (4 g, 10 mmol) were added over 30 minutes. The reaction mixture was stirred for 2 hours at 50 °C, and subsequently for an additional 24 to 48 hours at room temperature while monitoring the reaction status with TLC (2:98, ethylacetate:hexane). The final mixture was diluted with water (200 mL) and extracted with Et_2O (4×200 mL); the combined organic layers were washed with Brine solution (100 mL) and dried over $MgSO_4$, then filtered and concentrated under reduced pressure. The crude product was purified by chromatography on silica gel (hexane: EtOAc, 9.5:0.5 (v/v)) to provide 2-[(bis-methylthio)methylene]malononitrile with reasonable yields (75 %, 7.725 g). ^{1}H NMR (300 MHz, $CDCl_3$, 298 K, *δ (ppm)*): 2.76 (s, 6H, -SCH_3), Fig. S7. ^{13}C NMR (75 MHz, $CDCl_3$, 298 K, *δ (ppm)*): 184.0 (-C(S-Me)$_2$), 112.8 (-CN), 76.3 (-C(CN)$_2$), 19.3 (-SCH_3) (Fig. S8). IR data (ν, cm^{-1}): 3003w, 2926w, 2827w, 2417w, 2351w, 2308w, 2209s, 1489w, 1442s, 1417s, 1316m, 1211w, 983w, 960w, 922m, 869s, 708w, 610w, 475w, 457w (Fig. S9).

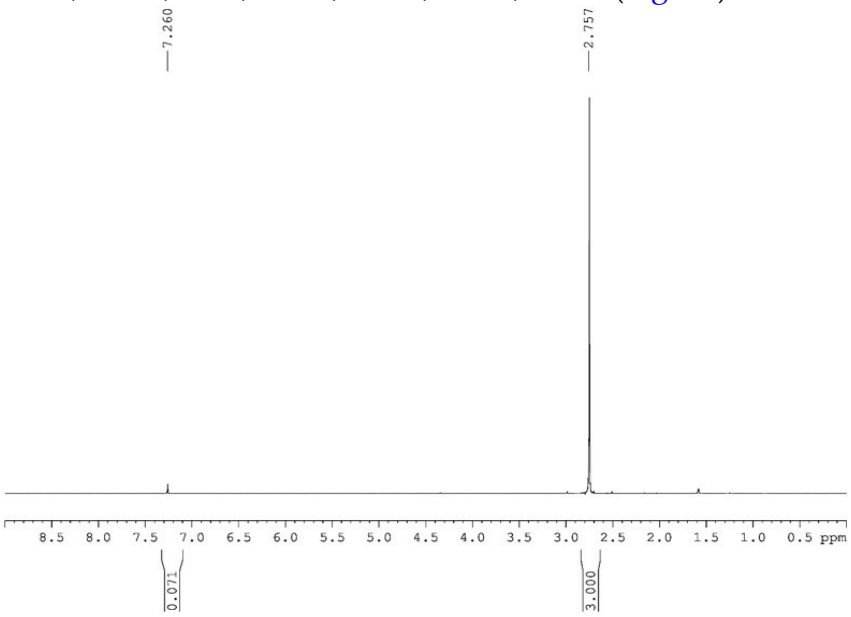

Figure S7. ^{1}H NMR (300 MHz, $CDCl_3$, 298K) of 2-[bis(methylthio)methylene]malononitrile.

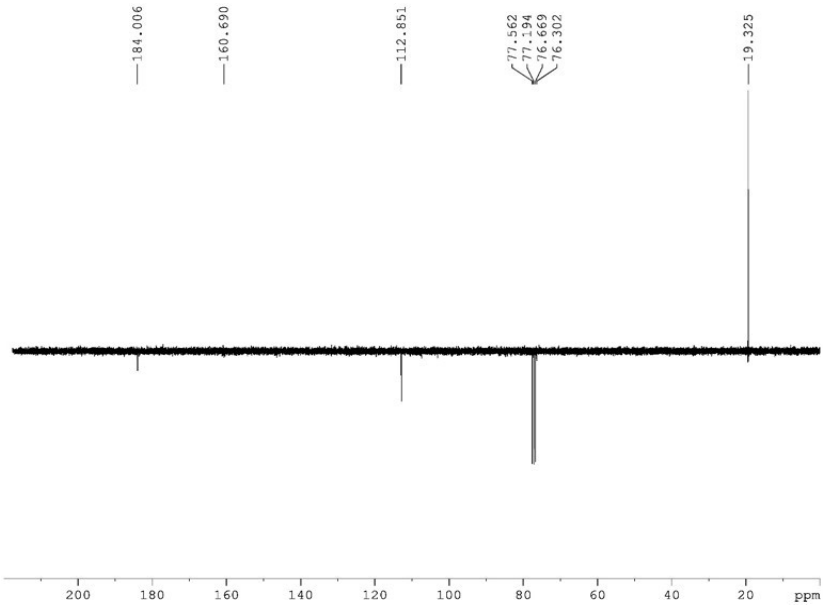

Figure S8. ^{13}C NMR (300 MHz, $CDCl_3$, 298K) of 2-[bis(methylthio)methylene]malononitrile

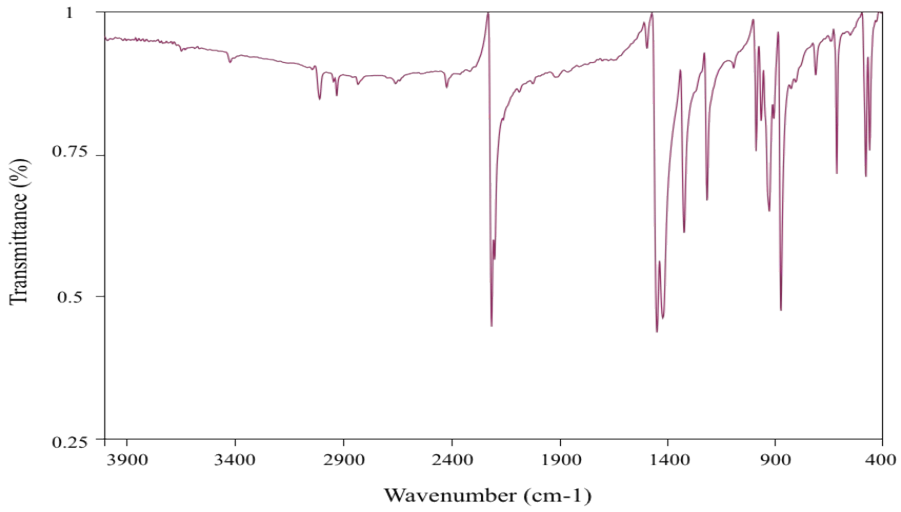

Figure S9. IR Spectrum of 2-[bis(methylthio)methylene]malononitrile.

(ii) Potassium 1,1,3,3-tetracyano-2-thiomethylpropenide salts (K(tcnsme)). A warm solution of the previously synthesized thioacetal, 2-[bis(methylthio)methylene]malononitrile (1.703 g, 10 mmol) in EtOH (30 mL), was added dropwise to an ethanol solution (10 mL) of malononitrile (0.66 g, 10 mmol) and t-BuOK (1.12 g, 10 mmol). The resulting solution was refluxed for 1h, and then the reaction mixture was cooled down to room temperature, and finally kept at 4 ^0C for two days. The resulting compound was filtered on a sintered-glass funnel and washed with distilled diethyl ether, and ultimately dried under vaccum to obtain yellow crystalline powders of K(tcnsme) salt in good yields (67 %, 1.516 g). ^1H NMR (300 MHz, Acetone-D_6, 298 K, δ

(ppm)): 2.54 (s, 3H -CH_3) (Fig. S10). ^{13}C NMR (125 MHz, Acetone-D_6, 298 K, *δ (ppm))*: 170.2 (-C(S-Me)$_2$), 119.0 (-CN), 117.0 (-CN), 53.6 (-C(CN)$_2$), 18.4 (-SCH_3), Fig. S11). IR data (ν, cm^{-1}): 2186s, 1447s, 1426m, 1332m, 1310m, 1247w, 956w, 929w, 856w, 642w, 576w, 527m, 473w (Fig. S12).

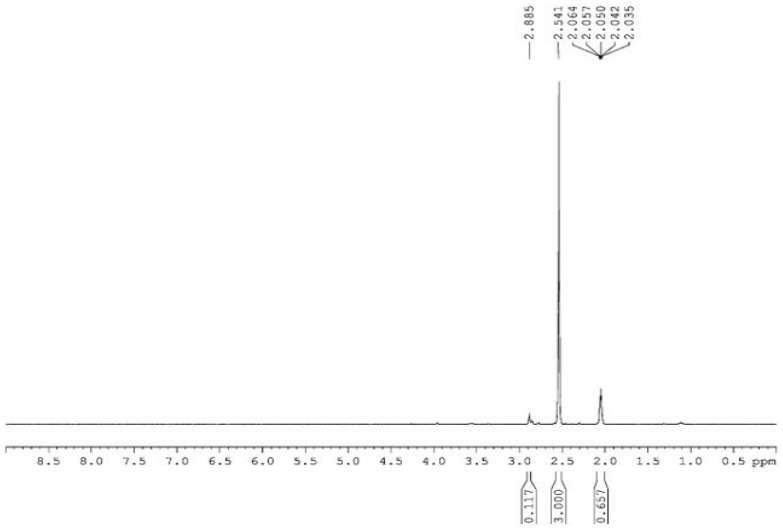

Figure S10. ^{1}H (300 MHz, Acetone-D_6) of K(tcnsme) at 298 K.

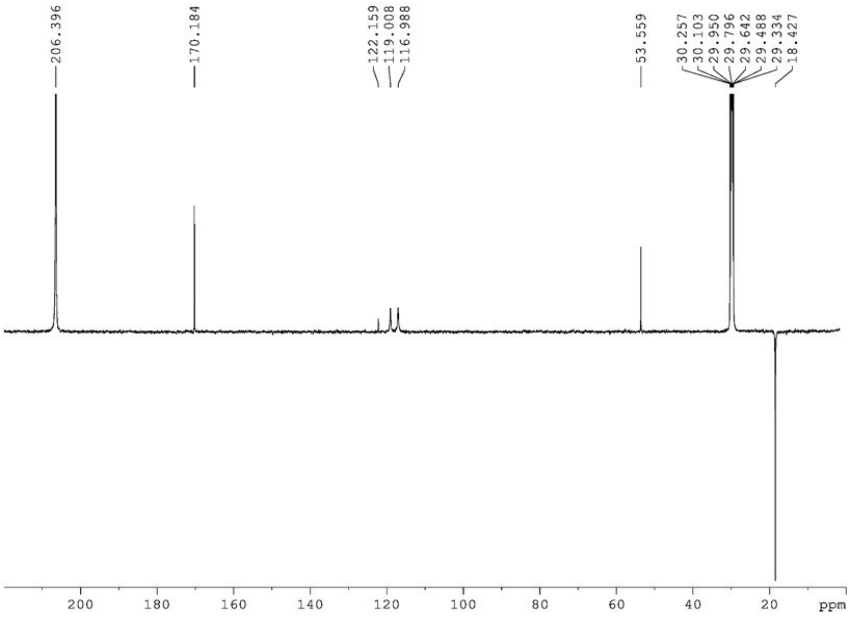

Figure S11. ^{13}CNMR (500 MHz, Acetone-D_6) of K(tcnsme) at 298 K.

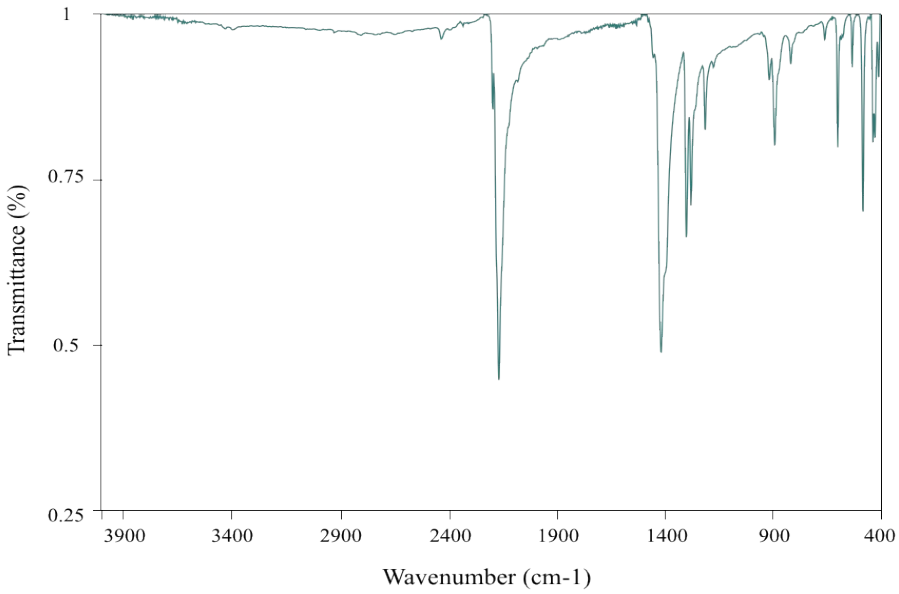

Figure S12. IR Spectrum of K(tcnsme).

3 - Synthesis of the $[Fe_3(\mu_2\text{-bntrz})_6(bntrz)_2(\mu_2\text{-tcnsme})_2](tcnsme)_4.4H_2O$ ($\mathbf{1\cdot 4H_2O}$) complex. A solution of bntrz (31.8 mg, 0.2 mmol) in 2.5 mL of distilled water and a solution of $Fe(BF_4)_2\cdot 6H_2O$ (33.755 mg, 0.1 mmol) and K(tcnsme) (45 mg, 0.2 mmol) in 10 mL of distilled water and acetone (1:1) with a pinch of ascorbic acid were prepared. Then, a solution of bntrz was put into a fine tube (5 mm diameter) and immediately covered with a small volume of water. Then, a solution of $Fe(BF_4)_2\cdot 6H_2O$ and K(tcnsme) in distilled water and acetone (1:1) was carefully layered on to the buffer solvent. Within 2 weeks in ambient conditions, micrometric needle shaped transparent yellow single crystals grew in urchin-like clusters at the interface of the solutions. Anal. Calcd. for $C_{120}H_{98}Fe_3N_{48}O_4S_6$ (**$\mathbf{1\cdot 4H_2O}$**): C, 54.7; N, 25.5; H, 3.7. Found: C, 55.0; N, 25.7; H, 3.5. IR data (see Fig. S13), ν/cm^{-1}: 3422br, 3138w, 3067w, 3065*w*, *2230w*, 2203s, 2187s, 1672w, 1636w, 1545m, 1454s, 1406 m, 1335m, 1312m, 1211m, 1180m, 1088m, 1028m, 1009w, 970w, 964w, 959w, 907m, 876m, 820w, 756w, 712s, 700m, 642s, 629m, 575m, 523m, 474m, 459 m 420w, 402w.

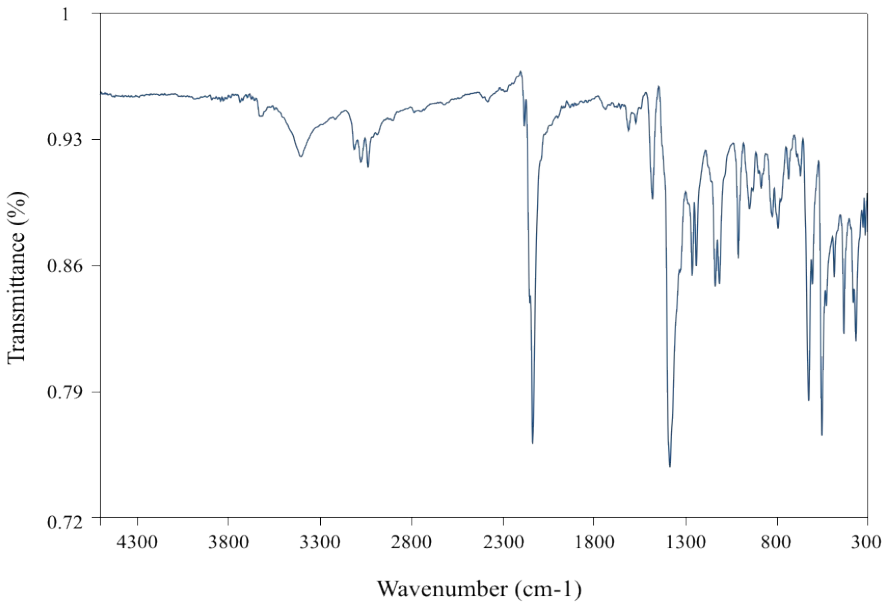

Figure S13. IR Spectrum of complex **1·4H$_2$O**.

4 – X-ray diffraction and structural characterization

The crystallographic studies of **1·4H$_2$O** were performed at room temperature (298 K) and at 150 K, using an Oxford Diffraction Xcalibur κ-CCD diffractometer equipped with a graphite monochromated Mo$K\alpha$ radiation (λ= 0.71073 Å). The full sphere data collections were performed using 1.0° ω-scans with different exposure times per frame (500 s at 298 K and 650 s at 150 K). Data collection and data reduction were done with the CRYSALIS-CCD and CRYSALIS-RED programs on the full set of data.[4] The crystal structures were solved by direct methods and successive Fourier difference syntheses, and were refined on F^2 by weighted anisotropic full-matrix least-square methods.[5] All non-hydrogen atoms were refined anisotropically and the hydrogen atoms were calculated and included as isotropic fixed contributors to F_c. All other calculations were performed with standard procedures (*OLEX2*).[6] Crystal data including structure refinement parameters, selected bond lengths and bond angles, and interchain contacts are listed in Tables S1-S3, respectively.

Table S1. Crystal data and structural refinement parameters for complex of $[Fe_3(bntrz)_8(tcnsme)_2](tcnsme)_4.4H_2O$ (**1·4H$_2$O**).

Complex	**1**	
Temperature (K)	298	150
Color	Yellow	Red
Formula	$C_{120}H_{98}Fe_3N_{48}O_4S_6$	
Radiation	MoKα (λ = 0.71073)	
M (g·mol^{-1})	2636.37	
Crystal system	Monoclinic	
Space group	$P2_1/n$	
a (Å)	14.073(1)	13.759(2)
b (Å)	22.411(1)	21.955(2)
c (Å)	21.028(2)	20.775(2)
β (°)	106.60(1)	106.06(1)
Volume (Å^3)	6355(1)	6031(1)
Z	2	
ρ_{calc} (g/cm^{-3})	1.378	1.452
Crystal size/mm^3	0.3375 × 0.0436 × 0.03	0.2125 × 0.03 × 0.02
μ (mm^{-1})	0.509	0.536
F(000)	2720	2720
2Θ range (°)	6.760 - 50.056	6.646 - 50.054
Reflections collected	27491	24617
R_{int}	0.1331	0.1792
Goodness-of-fit on F^2	0.941	0.908
R_1 / wR_2	0.0806 / 0.1342	0.0892/ 0.1705
Δρmax/min (e·Å^{-3})	0.35 /-0.33	0.50 / -0.40
Data/restraints/parameters	11186/0/820	10610/0/820

[a] $R1 = \sum |F_O - F_C| / F_O$. [b] $wR2 = \{w(F_o^2 - F_c^2)^2] / wF_o^2)^2]\}^{1/2}$. [c] $GooF = \{w(F_o^2 - F_c^2)^2] / (N_{obs} - N_{var})\}^{1/2}$

Table S2. Bond lengths and bond angles for $[Fe_3(bntrz)_8(tcnsme)_2](tcnsme)_4.4H_2O$ (**1·4H$_2$O**).

T/K	298K	150 K
Fe1-N1	2.044(5)	1.940(7)
Fe1-N2	2.048(5)	1.989(7)
Fe1-N3	2.048(5)	1.967(7)
Fe2-N4	2.113(5)	1.944(6)
Fe2-N5	2.151(5)	1.960(7)
Fe2-N6	2.147(5)	1.957(7)
Fe2-N7	2.135(5)	1.968(7)
Fe2-N8	2.145(6)	1.957(7)
Fe2-N9$^{(b)}$	2.105(6)	1.918(7)
N1-Fe1-N1$^{(a)}$	180	180
N1-Fe1-N2	91.8(2)	91.2(3)
N1-Fe1-N2$^{(a)}$	88.2(2)	88.8(3)
N1$^{(a)}$-Fe1-N2	88.2(2)	88.8(3)
N1$^{(a)}$-Fe1-N2$^{(a)}$	91.8(2)	91.2(3)
N1$^{(a)}$-Fe1-N3$^{(a)}$	92.7(2)	91.2(3)
N1-Fe1-N3$^{(a)}$	87.3(2)	88.8(3)
N1-Fe1-N3	92.7(2)	91.2(3)
N1$^{(a)}$-Fe1-N3	87.3(2)	88.8(3)
N2$^{(a)}$-Fe1-N2	180	180
N2$^{(a)}$-Fe1-N3	89.3(2)	90.3
N2-Fe1-N3$^{(a)}$	89.3(2)	90.3(3)
N2-Fe1-N3	90.7(2)	89.7(3)
N2$^{(a)}$-Fe1-N3$^{(a)}$	90.7(2)	89.7(3)
N3-Fe1-N3$^{(a)}$	180	180
N4-Fe2-N5	90.2(2)	91.9(3)
N4-Fe2-N6	91.1(2)	91.9(3)
N4-Fe2-N7	88.4(2)	87.3(3)
N4-Fe2-N8	88.8(2)	89.1(3)
N5-Fe2-N6	87.8(2)	88.7(3)
N5-Fe2-N7	178.1(2)	178.7(3)
N6-Fe2-N7	91.1(2)	90.3(3)
N7-Fe2-N8	91.0(2)	91.2(3)
N5-Fe2-N8	90.2(2)	89.8(3)
N6-Fe2-N8	177.9(2)	178.3(3)
N4-Fe2-N9$^{(b)}$	175.2(2)	173.5(3)
N5-Fe2-N9$^{(b)}$	90.6(2)	91.5(3)
N6-Fe2-N9$^{(b)}$	93.7(2)	93.6(3)
N7-Fe2-N9$^{(b)}$	90.9(2)	89.4(3)
N8-Fe2-N9$^{(b)}$	86.5(2)	85.5(3)

Codes of the equivalent positions: (a) -x, 1-y, -z; (b) 1-x, 1-y, -z.

Table S3. The shortest inter-chains contacts (C-H···N) observed for $[Fe_3(bntrz)_8(tcnsme)_2](tcnsme)_4.4H_2O$ (**1·4H$_2$O**). Such contacts involve aromatic C-H of the triazole moieties or C-H of the CH_2 group arising from the benzyl, and N atom from an isolated cyanocarbanion or a cyanocarbanion bonded to another chain.

D-H···A	d(D-H)/Å	d(H-A)/Å	d(D-A)/Å	D-H-A/°
Indirect contacts (via an isolated cyanocarbanion)				
C1-H1···N22	0.93	2.43	3.351(9)	171.0
C11-H11···N24[1]	0.93	2.59	3.304(10)	134.2
C20-H20···N21[2]	0.93	2.58	3.363(9)	141.9
C28-H28···N21[3]	0.93	2.38	3.139(9)	139.1
Direct contacts				
C30-H30a···N16[4]	0.97	2.58	3.337(10)	134.5

[1]-1/2-x,-1/2+y,-1/2-z; [2]-x,1-y,-z; [3]1+x,+y,+z; [4]1/2-x,-1/2+y,-1/2-z

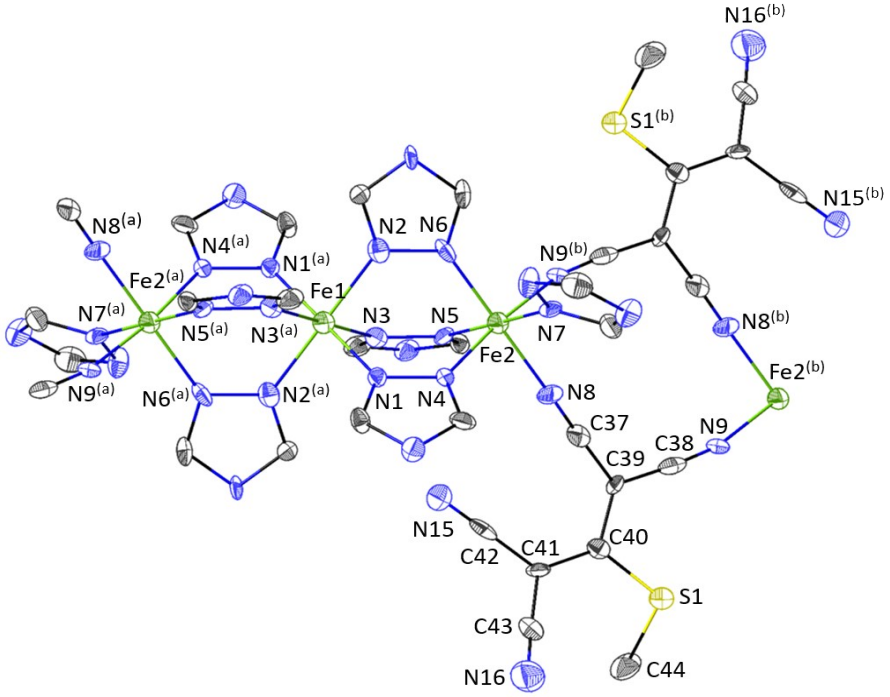

Figure S14. Molecular structure of **1·4H$_2$O** at 150 K, showing the atom labelling schemes and the coordination environments of the iron (II) ions. The benzyl group of the triazole ligand and all the hydrogen atoms have been omitted for the sake of clarity. Codes of the equivalent positions: (a) 1-x, 1-y, -z; (b) -x, 1-y, -z.

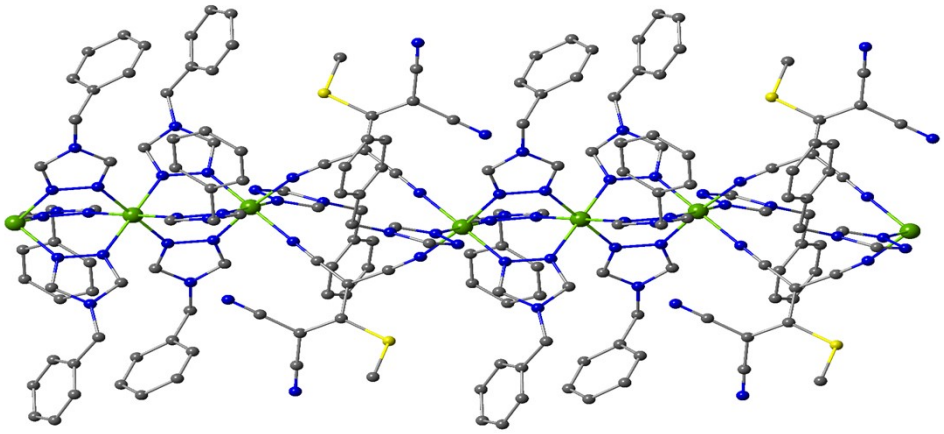

Figure S15. Structure of the one-dimensional coordination polymer of **1·4H$_2$O** at 150 K**.**

5 - Magnetic measurements. Variable temperature susceptibility measurements were carried out in the temperature range 50-370 K, with an applied magnetic field of 0.1 T, on polycrystalline samples of compound **1·4H$_2$O** (with mass of 25.02 mg) using a Quantum Design MPMS3 SQUID magnetometer. Experimental susceptibility was corrected for the diamagnetism of the constituent atoms of the sample by using Pascal's tables and the diamagnetism of the sample holder.[7] The sample was sealed in a double foil bag to protect it from solvent loss above room temperature in the vacuum condition of the SQUID magnetometer. The solvent loss still occurs at high temperature exceeding 345 K, but thanks to the use of the double foil bag it was possible to collect the magnetic data of **1·4H$_2$O** up to 345 K.

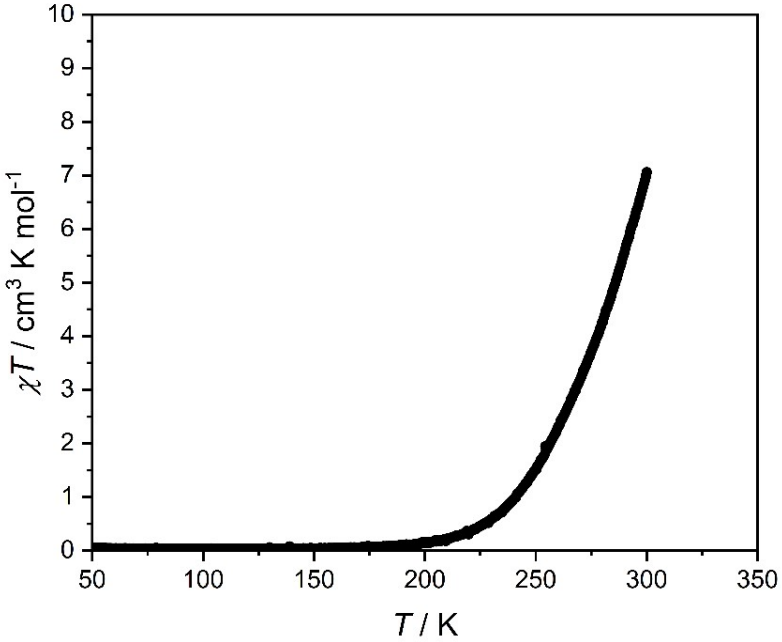

Figure S16. $\chi_m T(T)$ dependence obtained for **1·4H$_2$O** at 0.1 T using the photomagnetic setup (cooling rate 2 K min^{-1}).

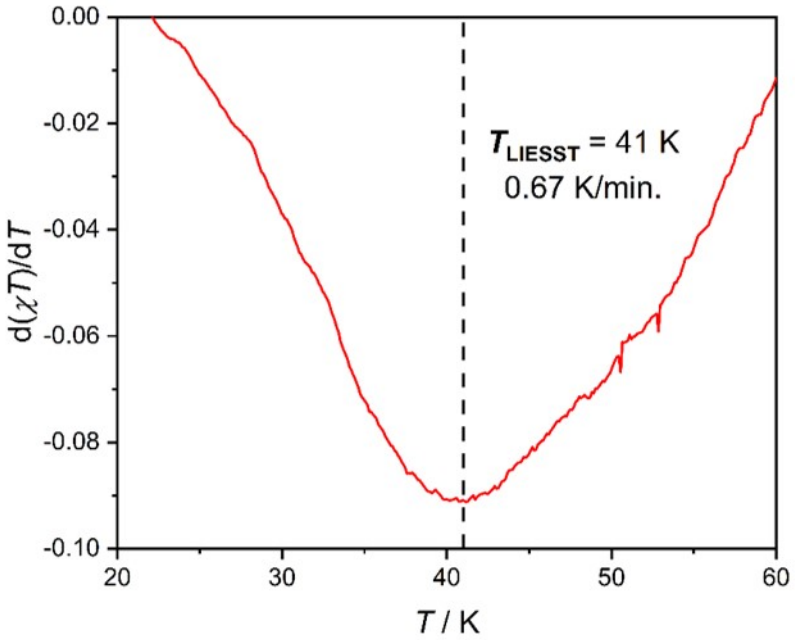

Figure S17. Thermal dependence of d($\chi_m T$)/dT derivative with the extremum corresponding to the T_{LIESST} of **1**.

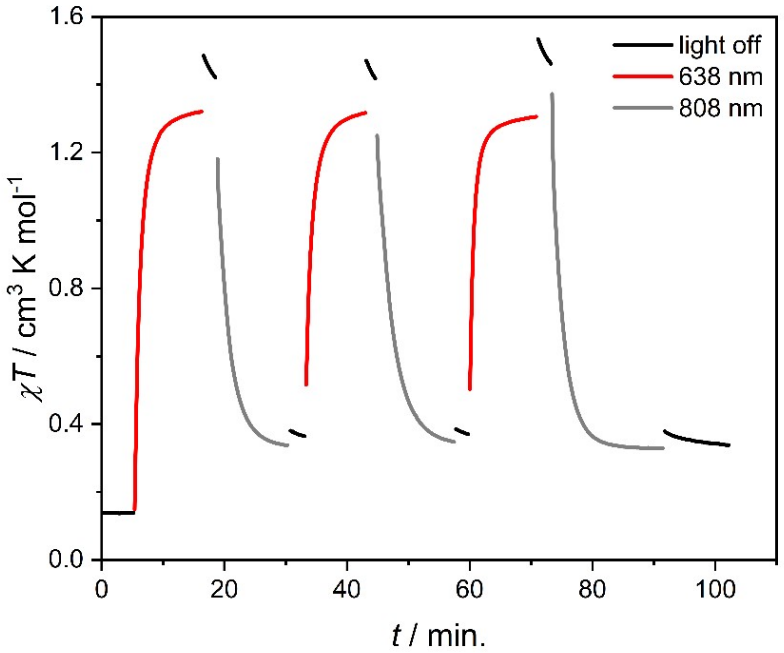

Figure S18. Three consecutive cycles of 638 nm - 808 nm irradiation recorded for **1** at 10 K and 0.1 T.

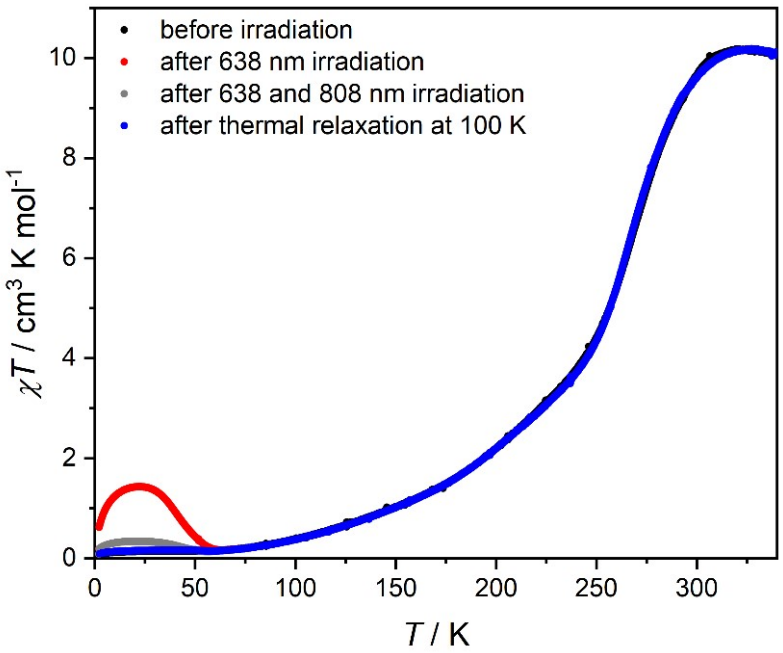

Figure S19. $\chi_m T(T)$ dependence obtained for **1** at 0.1 T before light irradiation (black), after 638 nm irradiation (red), after 638 nm irradiation followed by 808 nm light (grey) and after light irradiation followed by heating to 100 K (blue). Heating rate: 0.67 K min^{-1}; blue curve overlaps with the black one in entire measurement range.

6 – TGA analysis

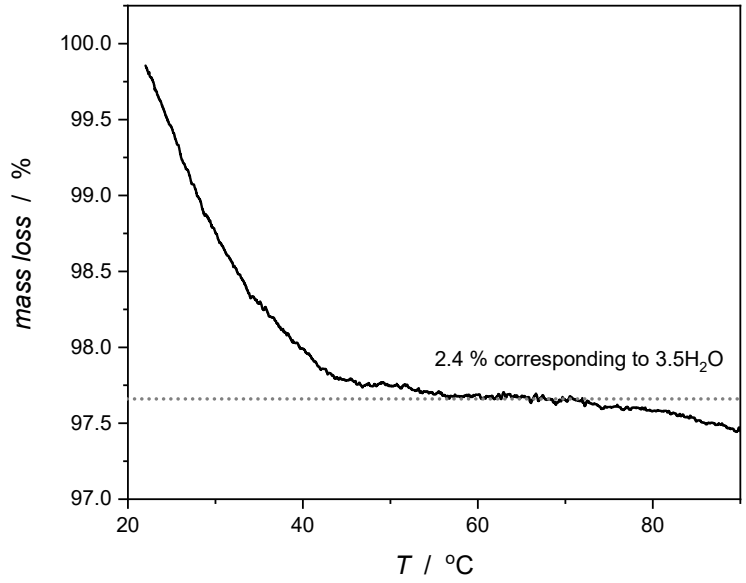

Figure S20. TGA analysis of compound **1·4H$_2$O.** The sample starts to lose weight from room temperature (20 °C) and loses 2.4 % of its mass when heated up to 60 °C.

7 -Magnetic and powder X-ray characterization of the hydrated (1·4H$_2$O) et the dehydrated (1) phases.

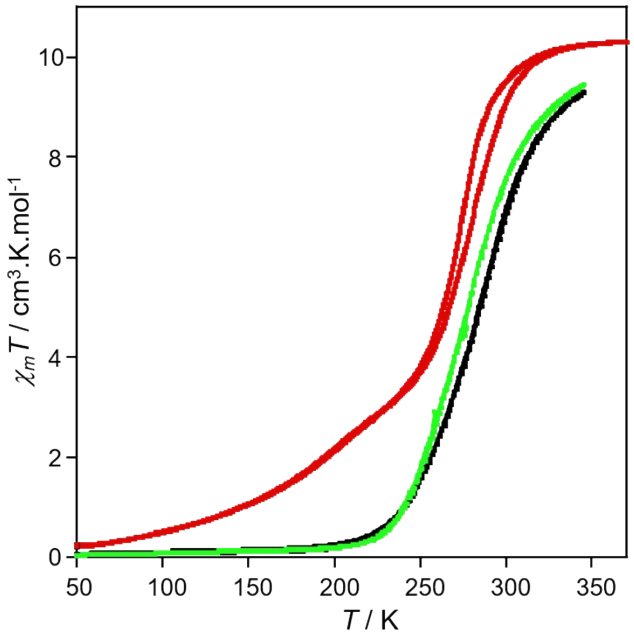

Figure S21. $\chi_m T(T)$ dependence at 0.1 T measured for **1·4H$_2$O** before dehydration (●), after dehydration (**1**) *in-situ* (●) and after rehydration (●) (**1·4H$_2$O**).

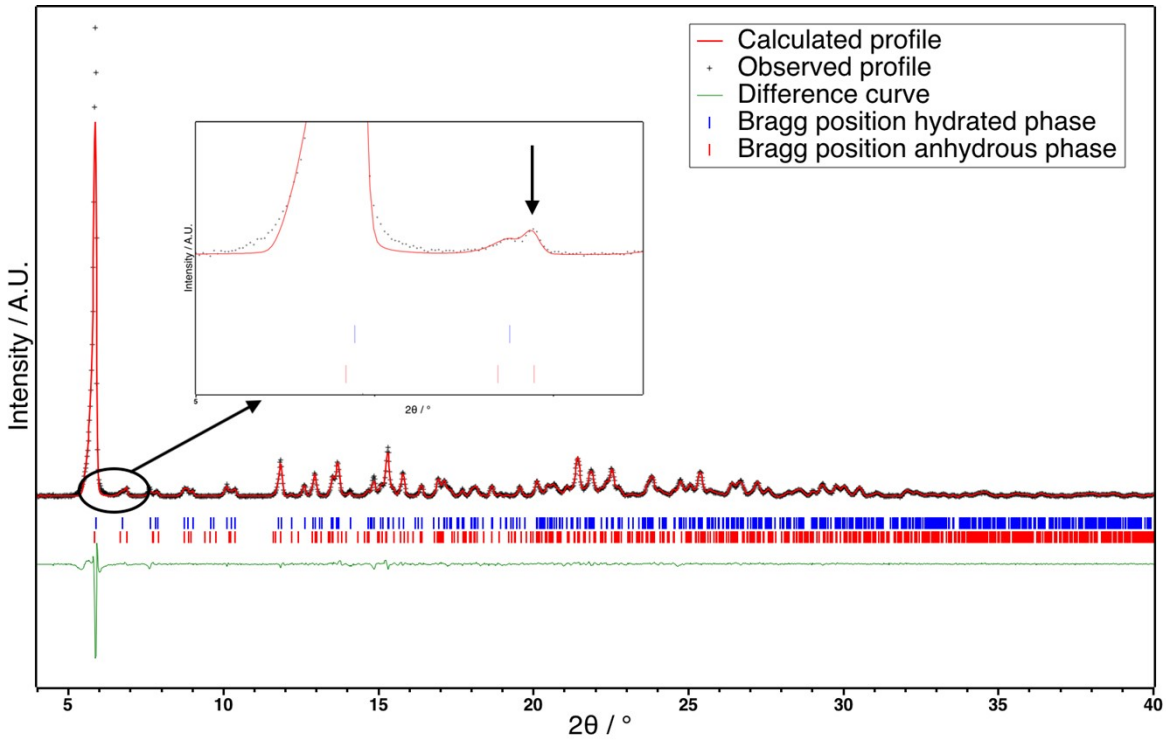

Figure S22. Rietveld refinement of the PXRD diagram of the hydrated phase (**1·4H$_2$O**). The inset is a zoom of the 5-8 ° region showing a small amount of anhydrous phase (black arrow).

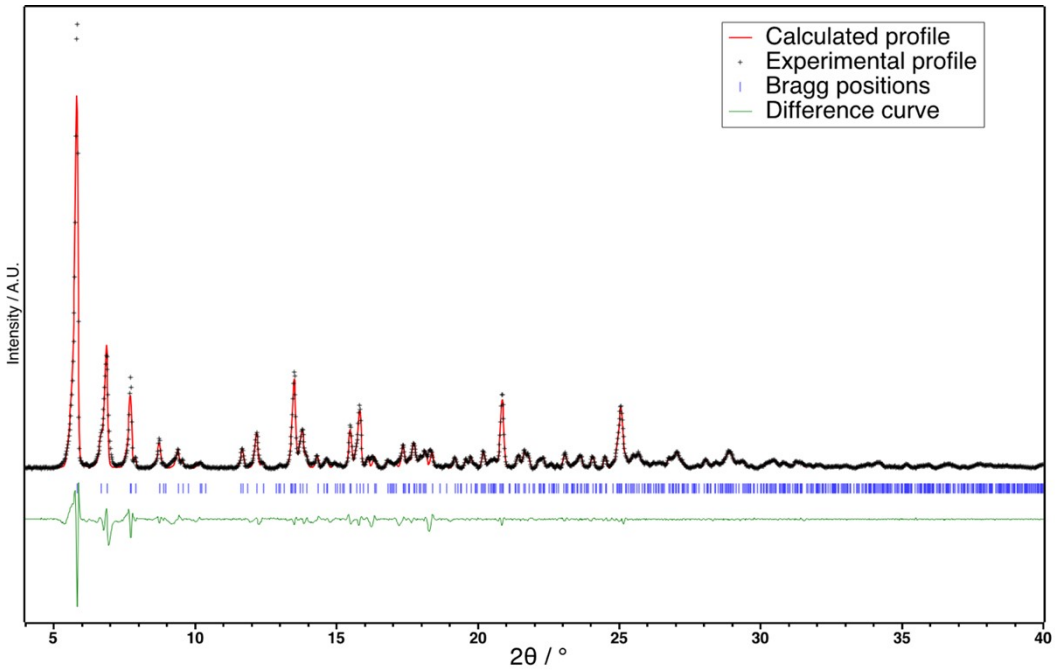

Figure S23. Profile matching of the PXRD diagram of the anhydrous phase (**1**) using the following unit cell parameter: a = 13.749 Å, b = 22.826 Å, c= 21.021 Å and β = 106.265.

8 -Infrared spectroscopy

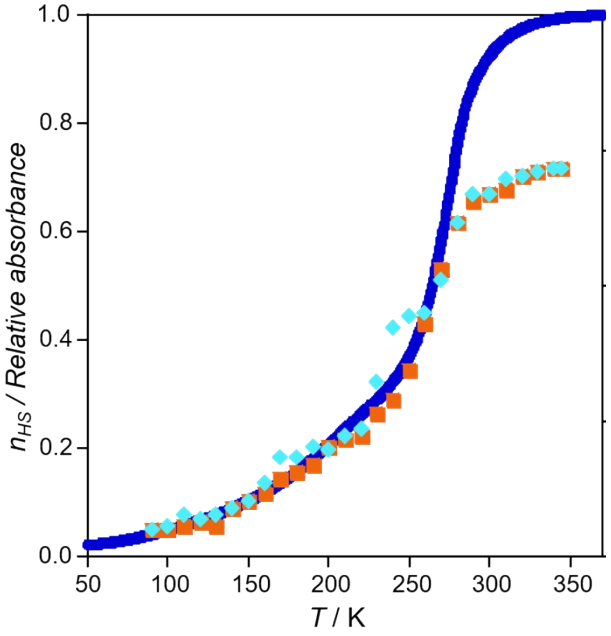

Figure S24. Temperature dependences of the relative absorbance of the ν(CN) bands observed at 2205 cm^{-1} (■) and at 2214 cm^{-1} (♦) in correlation with n_{HS} (●) derived from its magnetic properties for compound **1**.

References

1 N. Pittala, F. Thétiot, S. Triki, K. Boukheddaden, G. Chastanet and M. Marchivie, *Chem.Mater*., 2017, **29**, 490-494.

2 H. O. Bayer, R. S. Cook and W. C. Von Mayer, *US Patent*, 1974, 3821376.

3 N. Pittala, F. Thétiot, C. Charles, S. Triki, K. Boukheddaden, G. Chastanet and M. Marchivie, *Chem. Commun.*, 2017, **53**, 8356–8359.

4 CRYSALIS-CCD 170, Oxford-Diffraction (2002); CRYSALIS-RED 170, Oxford-Diffraction (2002).

5 A. Sheldrick, SHELX97. *Program for Crystal Structure Analysis*," University of Gottingen, Gottingen, Germany (1997).

6 O. V. Dolomanov, L. J. Bourhis, R. J. Gildea, J. A. K. Howard and H. Puschmann, *OLEX2: a complete structure, refinement and analysis program*, *J. Appl. Crystallogr.*, 2009, **42**, 339-341.

7 G. A. Bain and J. F. Berry, *J. Chem. Educ.*, 2008, **85**, 532-536.